

Quantification of cone loss after surgery for retinal detachment involving the macula using adaptive optics

M Saleh, G Debellemanière, M Meillat, P Tumahai, M Bidaut Garnier, M Flores, C Schwartz, B Delbosc

► Additional material is published online only. To view please visit the journal online (<http://dx.doi.org/10.1136/bjophthalmol-2013-304813>).

Department of Ophthalmology, University Hospital of Besançon, University of Franche-Comté, Besançon, France

Correspondence to

Dr M Saleh, Department of Ophthalmology, University Hospital of Besançon, University of Franche-Comté, CHU Jean Minjot, 3 Boulevard Fleming, Besançon 25030, France; msaleh@chu-besancon.fr

Received 30 December 2013

Revised 13 March 2014

Accepted 29 April 2014

ABSTRACT

Aims To image the cones in eyes with anatomically successful repair of retinal detachment (RD) involving the macula and in healthy fellow eyes using an adaptive optics (AO) camera and to correlate the results to clinical outcomes.

Methods Twenty-one patients (42 eyes) operated for macula-off RD were imaged 6 weeks after surgery using an AO camera (RTX 1, Imagine Eyes, Orsay, France). Cone density (cells/mm²), spacing between cells (μm) and the percentage of cones with six neighbours were measured. Best-corrected visual acuity (BCVA) and thickness of the inner segment ellipsoid (ISe) band imaged by SD-optical coherence tomography were also measured.

Results The parafoveal cone density was decreased in eyes operated for RD (mean±SD 14 576±4035/mm²) compared with fellow eyes (20 589±2350/mm²) (p=0.0001). There was also an increase in cone spacing (10.3±2.6 vs 8.0±1.0.9 μm, respectively, p<0.0001). The nearest-neighbour analysis revealed a reduction in the percentage of cones with six neighbours (36.5±4.2 vs 42.7±4.6%, p=0.0003). The ISe thickness, thinner in the operated eyes, was correlated to the cone density (r=0.62, p<0.0001). BCVA was significantly correlated to cone density (r=0.8, p<0.001).

Conclusions There was a decrease in the cone density after RD with an estimated loss of one-third of the cones. Postoperative visual acuity was highly correlated with the cone density. AO may be a valuable prognostic tool after RD surgery.

INTRODUCTION

Despite excellent surgical success rates, visual outcomes after rhegmatogenous retinal detachment (RD) involving the macula may still be disappointing.¹ To date, the precise cellular mechanisms that underlie the vision loss associated with RD are not completely understood.² However, the cone cell loss seems to be one of the major causes of poor vision in these patients. Photoreceptor apoptosis after RD has been reported in humans³ and in a variety of experimental models.^{4–6} Nevertheless, retinal cells are invisible using current standard imaging technologies, including optical coherence tomography (OCT) and scanning laser ophthalmoscopy (SLO).^{7–8} Instead, adaptive optics (AO) retinal imaging, which uses movable mirrors to compensate for aberrations in the optical path between the retina and the camera, allows direct visualisation of the living retina at a microscopic resolution. Recently, AO technology migrated from

fundamental research to various fields of clinical applications including imaging of epimacular membrane⁹ and macular hole.¹⁰ The development of commercially available compact devices is accelerating this transfer.^{11–12} In this study, we investigated cone loss ratio using AO in patients operated for RD and correlated the findings with postoperative clinical outcomes.

METHODS

Twenty-one adult patients (42 eyes) who underwent surgery for primary RD between July and November 2012 at the University Hospital of Besançon were studied. They all underwent 23-gauge vitrectomy with retinal tear cryoapplication and gas tamponade (20% SF6). Lens surgery with an aspherical intraocular lens was performed when needed. All patients underwent comprehensive ophthalmologic examinations at baseline and 6 weeks after the surgery, including best-corrected visual acuity (BCVA) (log-MAR), indirect ophthalmoscopy and axial length (IOL Master, Carl Zeiss Meditec, Dublin, California, USA).

In order to optimise image quality, patients with a known history of maculopathy, tear film disorder, opacities of the anterior segment and insufficient pharmacologically induced mydriasis (<5 mm) were excluded. The macula was examined to exclude patients displaying persistent subretinal fluid, macular oedema, epimacular membrane and large macular fold. Patients with spherical equivalent refractive error exceeding the spherical ametropia compensation range of the AO device (−12; +6D) were also excluded.

The protocol was approved by the local ethics committee and adhered to the tenets of Declaration of Helsinki. The nature of the study was explained to study candidates, after which written informed consent was obtained from all participants.

THE AO SYSTEM SPECIFICATIONS

Eyes were imaged using the RTX-1 AO device from Imagine Eyes (Orsay, France). This commercial clinical prototype is based on a non-coherent flood-illuminated design with an 850-nm central illumination wavelength with a 4°×4° imaging field of view (1.2×1.2 mm on the retina) and a focusing range of 600 μm, allowing high-resolution imaging of cones. Its low-noise CCD camera has a pixel resolution of 1.6 μm and a frame rate of 9.5 fps.

To cite: Saleh M, Debellemanière G, Meillat M, et al. *Br J Ophthalmol* Published Online First: [please include Day Month Year] doi:10.1136/bjophthalmol-2013-304813

IMAGE ACQUISITION PROCEDURE

AO imaging sessions were conducted after the pupils were dilated with one drop each of 0.5% tropicamide. The area of the retina to image was chosen by adjusting the position of the fixation target horizontally, and the imaging depth was chosen within the range of 0 to $-80\ \mu\text{m}$ (-800 and $+800\ \mu\text{m}$ corresponded to the anterior and posterior retina, respectively). In the device's control panel, a numerical value informed the operator on the level of AO correction. The acquisition lasted on average 1 min per eye.

IMAGE PROCESSING AND ANALYSIS

Each series of 40 images was processed using software programs provided by the system manufacturer (CK V0.1 and AOdetect V0.1, Imagine Eyes, France). These images were registered using a cross-correlation method¹³ and averaged to produce a final image with improved signal-to-noise ratio. The raw images that showed artefacts due to eye blinking and saccades were automatically eliminated before averaging. For display and printing purposes, the background of the resulting image was subtracted using a Gaussian filter and the histogram was stretched over a 16-bit range of grey levels.

The positions of photoreceptors were computed by automatically detecting the central coordinates of small circular spots whose brightness was higher than the surrounding background

level. First, the averaged image, as obtained before background removal and histogram stretching, was further processed using adaptive and multiple-scale digital filters. Then, the local maxima of the resulting filtered image were detected and their pixel coordinates were recorded. The spatial distribution of these point coordinates was finally analysed in terms of inter-cell spacing, local cell density and number of nearest neighbours using Delaunay triangulation and Voronoi diagrams.¹⁴ The area of analysis corresponded to two $90\text{-}\mu\text{m}$ squares ($0.3^\circ \times 0.3^\circ$) placed at a fixed distance from the fovea (2°), respectively, nasally and temporally along the horizontal axis of the eye studied (see online supplementary material 1). The data presented correspond to the mean of these two measurements.

INNER SEGMENT ELLIPSOID (ISE) BAND THICKNESS MEASUREMENTS

Spectral-domain OCT was performed using the Spectralis OCT (Heidelberg Engineering, Dossenheim, Germany). The protocol consisted of a 30° (length) horizontal line through the fovea with 1536 A-scans/B-scan. Twenty B-scans per image were averaged by the Tracking ART software with a resulting signal-to-noise ratio ≥ 25 dB. Images were evaluated independently by two readers (MS and GD), both unaware of clinical information. When the evaluations did not agree (difference $> 2\ \mu\text{m}$), the opinion of a third author (BD) was requested. In practice, on the Spectralis viewing module, the caller were manually moved to the borders of the ISe band previously called inner and outer segment junction (IS/OS) (see online supplementary materials 2 and 3). Recognising that, drawing the limits of the ISe layer on white on black images, lacked precision given the difficulty in differentiating subtle shades of grey, we selected the colour spectrum mode with a brightness set on 10 and a zoom to 225% (ISe corresponding to the red and/or white band). The thinnest point of the band in the corresponding AO area was determined. The reproducibility of the measurements was assessed. Data presented correspond to the mean of the ISe thickness measured nasally and temporally in each eye.

STATISTICAL ANALYSIS

All values represent the mean \pm SD. Wilcoxon matched-pairs signed-ranks test was used for statistical comparisons between groups, with the two-tail p value ≤ 0.05 considered significant. The non-parametric correlation with calculation of the Spearman's r was performed.

The degree of agreement between the two readers was assessed by the Bland-Altman method. Linear regression was performed with calculation of Pearson's correlation coefficient (r). The significance of Pearson's r was tested, with $p \leq 0.05$ considered significant. A multivariate stepwise linear regression was performed to determine which factors had a statistically significant effect (defined as $p \leq 0.05$) on cone density. The significant level at entry was 0.15 and for staying in the model was 0.05. Statistics were calculated using GraphPad InStat (GraphPad InStat, Inc, San Diego, California, USA). Linear and nonlinear regression graphs were obtained using Graph Prism 5 (GraphPad InStat, Inc).

RESULTS

All patients underwent anatomically successful RD repair. Exploitable AO images (figure 1) were obtained from all eyes except from two fellow eyes that displayed cataract.

The median time from onset of visual symptoms to RD surgery was 5 days, and median preoperative log-MAR visual

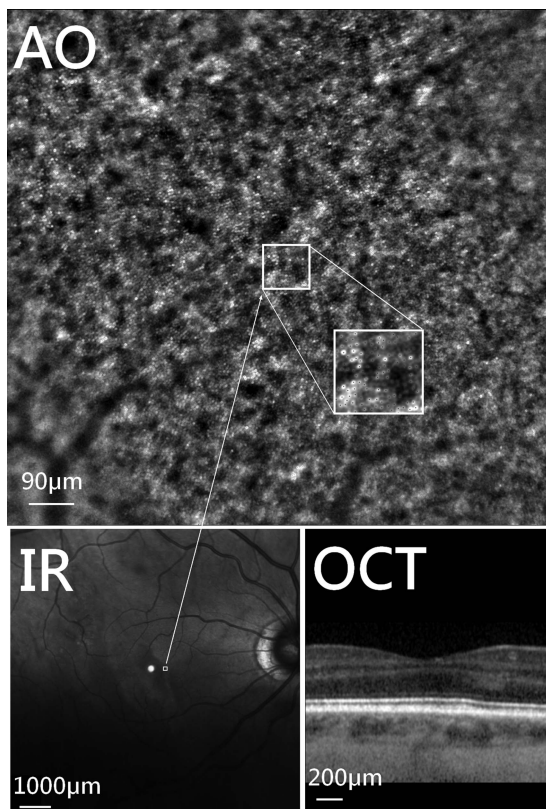


Figure 1 Patient who underwent macula-off retinal detachment repair in the right eye at the 6-week visit with a best-corrected visual acuity of 0.1 (logMAR). Top: adaptive optics (AO) image centred at 2° nasally from the centre of fovea showing a conservation of cone density (ie, 21 153 cells/ mm^2) and normal cone packing. Bottom: infrared image (IR) showing a small amount of extrafoveal subretinal fluid (blebs) and a normal spectral-domain optical coherence tomography (OCT) profile displaying a preservation of the photoreceptor inner and outer segment layers.

acuity was 2. (Baseline characteristics of eyes with RD with macular involvement and 6 weeks after surgical repair are summarised in online supplementary materials 4 and 5.)

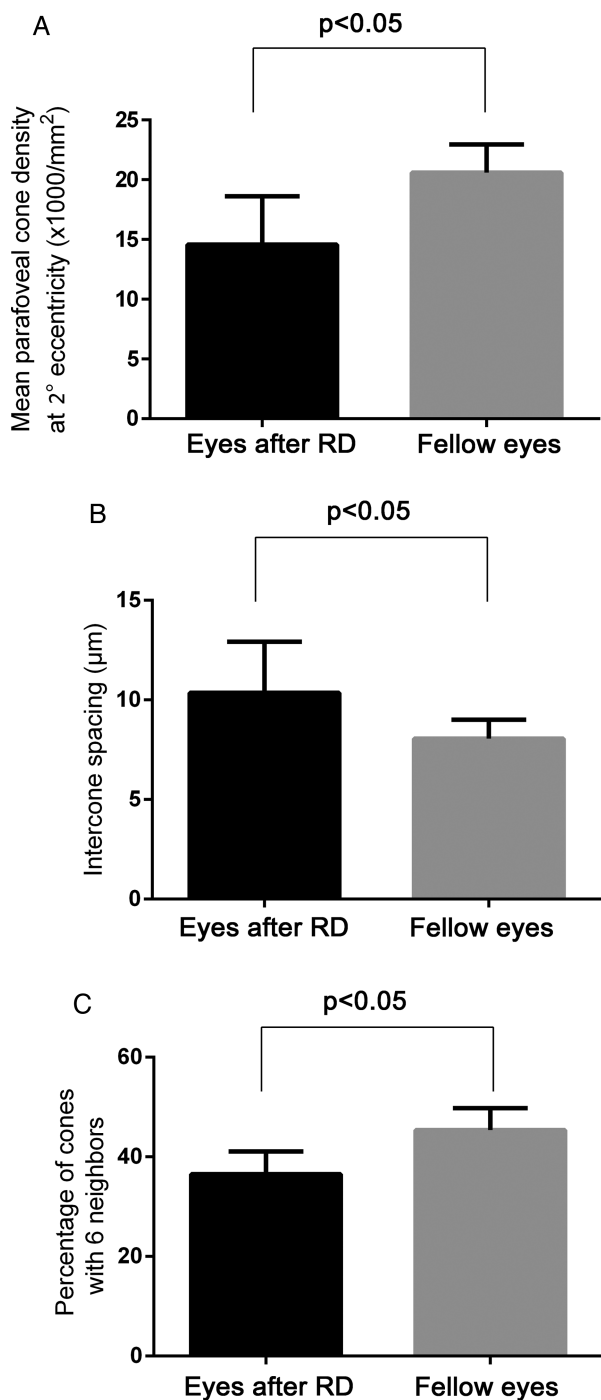


Figure 2 (A) Mean parafoveal cone density at the 6-week visit (mean±SD). Eyes that underwent retinal detachment (RD) surgery displayed a decrease in cone density compared with fellow eyes (matched-pairs test, $p=0.0001$). (B) Mean parafoveal spacing between cones at the 6-week visit (mean±SD). Eyes that underwent RD surgery displayed an increase in intercone spacing compared with fellow eyes (matched-pairs test, $p<0.0001$). (C) Mean percentage of cones with six neighbours calculated on Voronoï diagrams (mean±SD). Eyes that underwent RD surgery displayed a disorganisation of the cone mosaic compared with fellow eyes (matched-pairs test, $p=0.0003$).

Surgical treatment of RD significantly improved mean visual acuity (matched-pairs test, $p<0.0001$). At the 6-week visit, the AO imaging revealed decreased cone density in all operated eyes but one compared with fellow eyes ($p=0.0004$). The mean decrease reached 31%. There was also an increase in cone spacing ($p<0.0001$) in these eyes of 30.9% in average. The results of the nearest-neighbour analysis revealed that eyes with a history of RD also had fewer cones with six neighbours, which is a sign of the cone mosaic disorganisation ($p=0.0015$) (figure 2).

Structural changes took place in a similar proportion in the nasal and temporal areas ($p>0.05$) (see online supplementary material 6).

SD-OCT analysis revealed ISe band defects (thinning, hypoflectivity and/or pigment migrations) in the parafoveal area of eyes operated for RD in 80.9% of cases (Fisher's exact test, $p<0.0001$). Despite the difficulty encountered in some cases to delineate the boundaries of the ISe band, regardless of the display mode of the OCT scan (either in black and white or in colour), the reproducibility of the ISe thickness measurements appeared to be acceptable for the purpose of the study with an excellent agreement between the two readers (difference $\leq 2 \mu\text{m}$) in 41% of the cases (linear regression, $r^2=0.72$) (see online supplementary material 7) and an average bias provided by the Bland-Altman analysis of $-0.64 \mu\text{m}$ (95% CI -6.15 to $4.85 \mu\text{m}$) (see online supplementary material 8). The ISe thickness median was $17 \mu\text{m}$ in the operated eyes and was overall correlated to cone density in the corresponding foveal area (Spearman's $r=0.58$, $p=0.0005$) (see online supplementary material 9). Foveal thickness was comparable in both groups at the 6-week visit. The different pattern of cone loss is shown in figure 3.

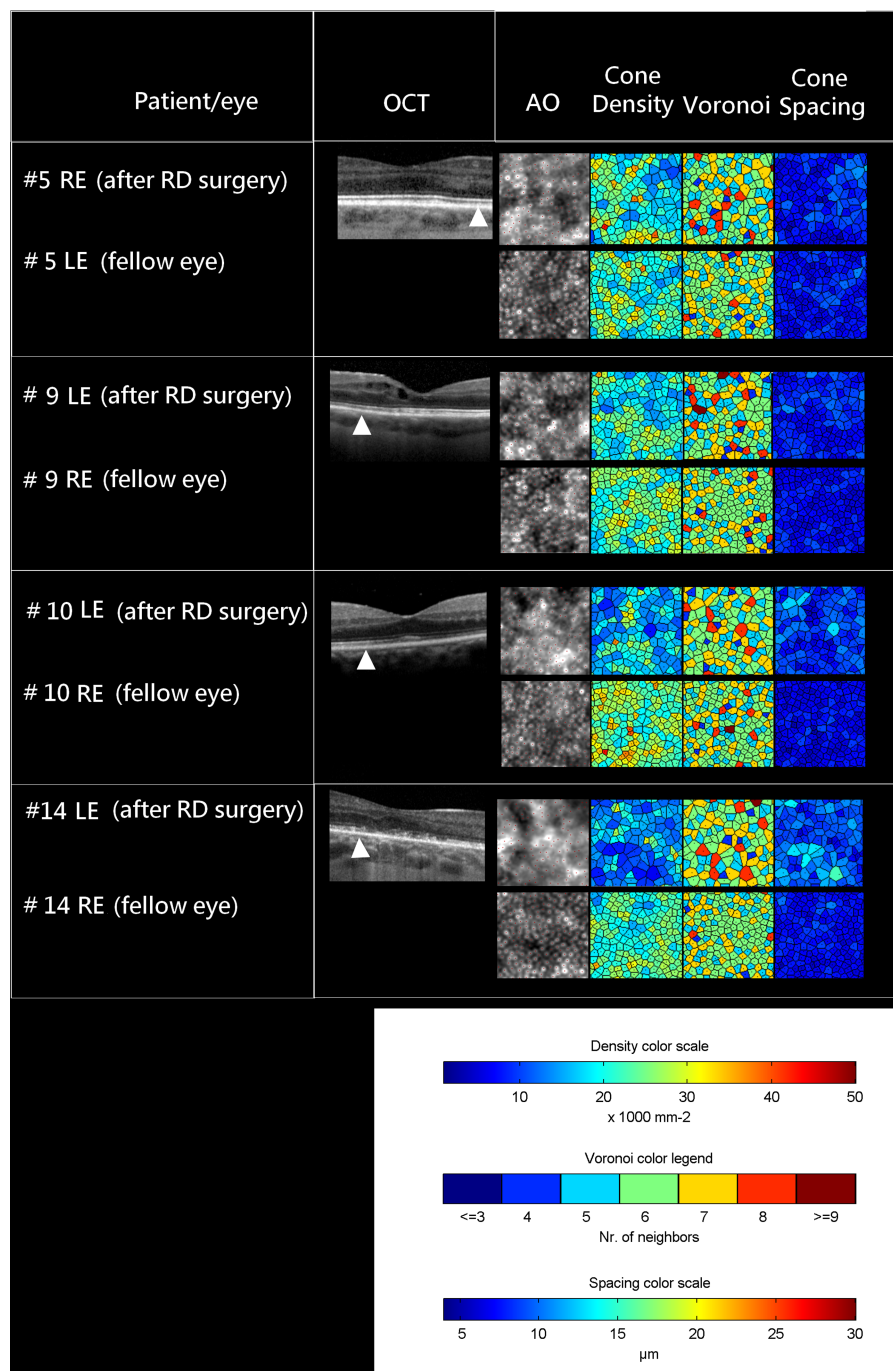
BCVA was strongly correlated to cone density ($|\text{Spearman's } r|=0.8$, $p<0.0001$) (see online supplementary material 10) and inversely correlated to intercone spacing, and in a lesser proportion to the percentage of cones with six neighbours (see online supplementary material 11). Multivariate regression analysis showed a significant correlation of the cone density with several factors (see online supplementary material 12): in this model, preoperative VA, foveal height, presence and duration of RD explained 70.1% of the cone density variability.

DISCUSSION

Because of the scarcity of human tissue samples, much of the knowledge concerning the histological features and pathophysiology of RD comes from animal studies. AO technology opens a new frontier for the research in retinal pathology in human eyes. According to a Medline search, this is the first report to use AO to quantify, qualitatively and quantitatively, changes in the macular cones and to correlate the results with visual acuity, a macular task, after anatomically successful repair of rhegmatogenous RDs.

Cones were imaged at 2° of eccentricity and not closer to the centre because cells appear blurred in the foveola due to resolution limitation of the AO camera (see online supplementary material 1). At that distance, the intersubject variability in photoreceptor density is reduced, which makes comparisons between patients more relevant. It should be also noted that photoreceptors in this area are still mostly cones,¹⁵ reducing the risk of confusion with rods during the automated detection of cones by the software. Taking into account that it is not possible to count photoreceptors before surgery in the presence of sub-retinal fluid (see online supplementary material 13), we took the fellow eye as a reference to investigate cone loss ratio after RD.

Figure 3 Progressive pattern of cone loss observed in eyes operated for retinal detachment and comparison with the normal fellow eyes (top to down). Arrows pointing at spectral-domain-optical coherence tomography (OCT) profiles correspond to the areas of adaptive optics (AO) imaging. Cone density, packing and spacing maps provided by 'AO detect 0.1' software are shown with the corresponding colour scale for interpretation. Incremental loss of cones was associated to various defects of the ISe band on SD-OCT (#5: normal ISe; #9: thinned ISe; #10: thinned and hyporeflective ISe; #14: disrupted ISe). Overall, in operated eyes, there was a decrease in cone density, an increase in intercellular spacing and a decrease in the rate of cones with six neighbours (disorganisation of the cone mosaic) (matched-pairs test, $p < 0.05$). RE, right eye; LE, left eye.



A histological study has shown that variation in two normal fellow eye cone and rod numbers is usually within 8%.¹⁶ Lombardo *et al*¹⁷ also showed that the cone density followed a symmetrical distribution between fellow eyes and that despite significant intersubject variability, the intrasubject variation of cone density was moderate (coefficient of variation $\leq 13\%$ in 95% of the subject variability). In this study, one patient displayed a higher cone density in the operated eye. In fact, although the intrasubject SD in the Lombardo *et al* study was overall reduced (1600 cones/mm² at 760 µm), one of their 20 healthy volunteers showed a greater interocular asymmetry (of approximately 5000 cones/mm²). Thus, a pre-existing cone density asymmetry within normal range and exceeding the cone loss caused by the RD, even if it is still possible, seems infrequent.

Imaging with AO after RD surgery has overall demonstrated a loss of cones, an increase in spacing between cells and a modification of the cone packing.

In experimental models, the photoreceptor loss has been correlated to the retinal functional changes including impairment of the ERG responses.¹⁸ In the current study, we found a high correlation between the cone density and the postoperative visual acuity. Patients who presented a clinically measurable visual loss after RD repair (defined as a difference of more than 0.1 logMAR between both eyes) are those who lost, at least, one-third of their cones (figure 4). Strikingly, a recent work on AO after macular hole closures also underlines a ratio of cone loss exceeding one-third in order to observe a decrease in visual acuity.¹⁹ Most of the apoptotic changes observed after RD are limited to the outer nuclear layer with a relative conservation of

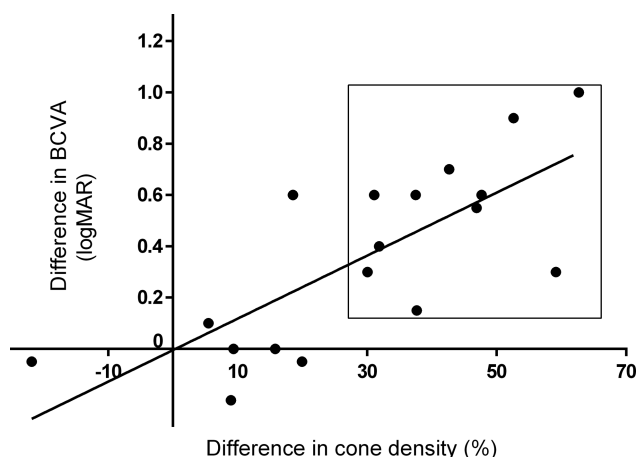


Figure 4 Comparison between eyes that presented retinal detachment (RD) and fellow eyes. There was a linear relationship between the difference in cone density and the difference in visual acuity ($r^2=0.56$, $p=0.0003$). Patients who presented a clinically measurable visual loss after RD repair (defined as a difference of more than 0.1 logMAR) are those that lost at least one-third of their parafoveal cones (square).

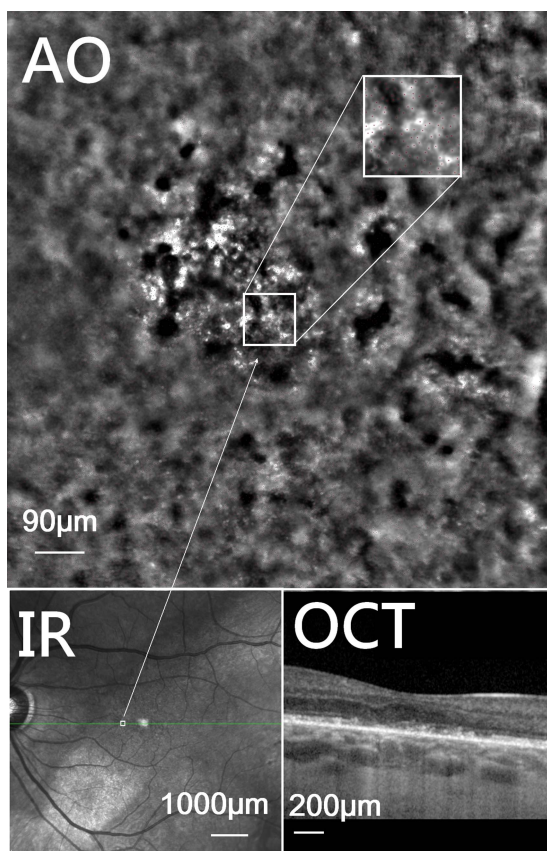


Figure 5 Patient who underwent macula-off retinal detachment repair in the left eye at the 6-week visit with a final best-corrected visual acuity of 0.4 (logMAR). Top: adaptive optics (AO) image centred at 2° nasally from the fovea showing a cone loss (ie, 12 052 cells/mm²) and a modification of the cone packing compared with the fellow eye (not shown). Cell polymegathism is also observed. Bottom: infrared image (IR) showing an extensive retinal scar. The B-scan on spectral-domain optical coherence tomography (OCT) shows severe ISe band disruption.

the other layers.^{20 21} This is corroborated by OCT studies^{7 8} that suspected dropout of the foveal photoreceptor inner and outer segment layers to be a key feature responsible for incomplete postoperative recovery of visual acuity. Considering that OCT ISe band and AO retinal imaging are based on the reflectivity of the cone outer segment tips, it is not surprising that we observed a good correlation between both measures. This finding confirms the previously reported prognostic value of outer retinal layer integrity in macular conditions.^{22 23} Similarly, it has been shown recently that foveolar cone loss on AO-SLO correlated also with thinner ISe band after surgical closure of macular hole.¹⁹

On a qualitative note, cone packing modifications were observed in operated eyes. One eye with extensive postoperative retinal scarring also showed increased cell size (figure 5). Even if polymegathism has been reported in RPE,²⁴ this is not a common feature of apoptotic cones. One possible explanation could be that cone pedicles lose some of the complex synaptic invaginations that populate their base, resulting in a flattened appearance,² with a resulting greater reflectance on AO. However, this study was not designed to investigate cellular morphology. Ooto *et al*²⁵ studied the pathological changes in photoreceptors in eyes with resolved central serous chorioretinopathy (CSC) using an AO-SLO device. They observed abnormal cone mosaic patterns and reduced cone densities in eyes with resolved CSC, and these abnormalities were associated with VA loss and disruptions in the ISe band or in the intermediate line on SD-OCT images. They also observed in some patients, but not all, highly reflective irregular patches of mosaic and dark regions where cones were missing or damaged. Such dark regions were present, at various levels, in all the operated eyes of this study (figure 5), probably contributing to the poorer visual prognosis after macula-off rhegmatogenous RD.

This study has limitations. The device did not allow to properly investigate the foveola, where the relationship between structure and function, highlighted in the parafoveal area, may be reinforced. Another major concern was to underestimate the cone density by including AO images of poor quality. To avoid this pitfall, a number of constraints were observed: the index of live correction of aberrations displayed during the image acquisition was taken into account. In addition, several images were taken and the one displaying the sharpest central area was selected for measurement. We also relied on the OCT signal-to-noise ratio to select the patients with the clearest media. As a result, only half of the potential candidates were eventually included. Another limitation includes the cross-sectional design. AO imaging before 6 weeks was not possible due to the presence of gas that compromised signal acquisition. Apoptosis is an evolutive process, and a cellular count at a single time point could miss changes that could appear later. Nevertheless, most of the photoreceptor loss has already taken place at this time limit.²⁶ Long-term follow-up would add valuable information on the natural history of cone death. Recently, potential therapeutic targets for rescuing the photoreceptors, such as oxygen supplementation, delivery of neurotrophic factors and blockage of protein activity,² were developed. In the future, AO imaging, alone or combined with another technique of imaging,²⁷ could help monitoring the results in humans.

CONCLUSION

AO allowed objective assessment of cone loss after RD surgery. Further studies are needed to define potential applications in a clinical setting.

Contributors Substantial contributions to conception and design: MS and BD; acquisition of data: MS, GD, MM, PT, MBG, MF and CS; analysis and interpretation of data: MS, GD, PT, MBG and MF; drafting the article: GD, MM, PT, MF and CS; revising it critically for important intellectual content: MS, MBG and BD; and final approval of the version to be published: all authors.

Funding This work was supported by AFCRO grant number 130712. No additional external funding was received for this study.

Competing interests None.

Patient consent Obtained.

Ethics approval Comité d'éthique du Pole chirurgie.

Provenance and peer review Not commissioned; externally peer reviewed.

REFERENCES

- Burton TC. Recovery of visual acuity after retinal detachment involving the macula. *Trans Am Ophthalmol Soc* 1982;80:475–97.
- Kubay OV, Charteris DG, Newland HS, *et al*. Retinal detachment neuropathology and potential strategies for neuroprotection. *Surv Ophthalmol* 2005;50:463–75.
- Chang CJ, Lai WW, Edward DP, *et al*. Apoptotic photoreceptor cell death after traumatic retinal detachment in humans. *Arch Ophthalmol* 1995;113:880–6.
- Fisher SK, Lewis GP, Linberg KA, *et al*. Cellular remodeling in mammalian retina: results from studies of experimental retinal detachment. *Prog Retin Eye Res* 2005;24:395–431.
- Linberg KA, Sakai T, Lewis GP, *et al*. Experimental retinal detachment in the cone-dominant ground squirrel retina: morphology and basic immunocytochemistry. *Vis Neurosci* 2002;19:603–19.
- Machemer R. Experimental retinal detachment in the owl monkey. II. Histology of retina and pigment epithelium. *Am J Ophthalmol* 1968;66:396–410.
- Lecleire-Collet A, Muraine M, Menard JF, *et al*. Evaluation of macular changes before and after successful retinal detachment surgery using stratus-optical coherence tomography. *Am J Ophthalmol* 2006;142:176–9.
- Wakabayashi T, Oshima Y, Fujimoto H, *et al*. Foveal microstructure and visual acuity after retinal detachment repair: imaging analysis by Fourier-domain optical coherence tomography. *Ophthalmology* 2009;116:519–28.
- Ooto S, Hangai M, Takayama K, *et al*. High-resolution imaging of the photoreceptor layer in epiretinal membrane using adaptive optics scanning laser ophthalmoscopy. *Ophthalmology* 2011;118:873–81.
- Ooto S, Hangai M, Takayama K, *et al*. Photoreceptor damage and foveal sensitivity in surgically closed macular holes: an adaptive optics scanning laser ophthalmoscopy study. *Am J Ophthalmol* 2012;154:174–86.
- Gocho K, Sarda V, Falah S, *et al*. Adaptive optics imaging of geographic atrophy. *Invest Ophthalmol Vis Sci* 2013;54:3673–80.
- Lombardo M, Parravano M, Lombardo G, *et al*. Adaptive optics imaging of parafoveal cones in type 1 diabetes. *Retina* 2014;34:546–57.
- Zitova B, Flusser J. Image registration methods: a survey. *Image Vision Comput* 2003;21:977–1000.
- Li KY, Tiruveedhula P, Roorda A. Intersubject variability of foveal cone photoreceptor density in relation to eye length. *Invest Ophthalmol Vis Sci* 2010;51:6858–67.
- Purves D, Augustine GJ, Fitzpatrick D. Anatomical distribution of rods and cones. In: Dale Purves, George J Augustine, David Fitzpatrick, Lawrence C Katz, Anthony-Samuel LaMantia, James O McNamara, and S Mark Williams, eds. *Neuroscience*. Sunderland (MA): Sinauer Associates; 2001.
- Curcio CA, Sloan KR, Kalina RE, *et al*. Human photoreceptor topography. *J Comp Neurol* 1990;292:497–523.
- Lombardo M, Lombardo G, Schiano Lomoriello D, *et al*. Interocular symmetry of parafoveal photoreceptor cone density distribution. *Retina* 2013;33:1640–9.
- Hisatomi T, Sakamoto T, Goto Y, *et al*. Critical role of photoreceptor apoptosis in functional damage after retinal detachment. *Curr Eye Res* 2002;24:161–72.
- Yokota S, Ooto S, Hangai M, *et al*. Objective assessment of foveal cone loss ratio in surgically closed macular holes using adaptive optics scanning laser ophthalmoscopy. *PLoS ONE* 2013;8:e63786.
- Arroyo JG, Yang L, Bula D, *et al*. Photoreceptor apoptosis in human retinal detachment. *Am J Ophthalmol* 2005;139:605–10.
- Guerin CJ, Lewis GP, Fisher SK, *et al*. Recovery of photoreceptor outer segment length and analysis of membrane assembly rates in regenerating primate photoreceptor outer segments. *Invest Ophthalmol Vis Sci* 1993;34:175–83.
- Shimozono M, Oishi A, Hata M, *et al*. The significance of cone outer segment tips as a prognostic factor in epiretinal membrane surgery. *Am J Ophthalmol* 2012;153:698–704.
- Itoh Y, Inoue M, Rii T, *et al*. Correlation between length of foveal cone outer segment tips line defect and visual acuity after macular hole closure. *Ophthalmology* 2012;119:1438–46.
- Brown J Jr, Hacker H, Schuschereba ST, *et al*. Steroidal and nonsteroidal antiinflammatory medications can improve photoreceptor survival after laser retinal photocoagulation. *Ophthalmology* 2007;114:1876–83.
- Ooto S, Hangai M, Sakamoto A, *et al*. High-resolution imaging of resolved central serous chorioretinopathy using adaptive optics scanning laser ophthalmoscopy. *Ophthalmology* 2010;117:1800–9.
- Anderson DH, Guerin CJ, Erickson PA, *et al*. Morphological recovery in the reattached retina. *Invest Ophthalmol Vis Sci* 1986;27:168–83.
- Podoleanu AG, Rosen RB. Combinations of techniques in imaging the retina with high resolution. *Prog Retin Eye Res* 2008;27:464–99.



Quantification of cone loss after surgery for retinal detachment involving the macula using adaptive optics

M Saleh, G Debellemanière, M Meillat, et al.

Br J Ophthalmol published online June 3, 2014
doi: 10.1136/bjophthalmol-2013-304813

Updated information and services can be found at:
<http://bjo.bmj.com/content/early/2014/06/03/bjophthalmol-2013-304813.full.html>

These include:

Data Supplement

"Supplementary Data"

<http://bjo.bmj.com/content/suppl/2014/06/04/bjophthalmol-2013-304813.DC1.html>

References

This article cites 25 articles, 4 of which can be accessed free at:
<http://bjo.bmj.com/content/early/2014/06/03/bjophthalmol-2013-304813.full.html#ref-list-1>

P<P

Published online June 3, 2014 in advance of the print journal.

Email alerting service

Receive free email alerts when new articles cite this article. Sign up in the box at the top right corner of the online article.

Topic Collections

Articles on similar topics can be found in the following collections

[Retina](#) (1379 articles)

Advance online articles have been peer reviewed, accepted for publication, edited and typeset, but have not yet appeared in the paper journal. Advance online articles are citable and establish publication priority; they are indexed by PubMed from initial publication. Citations to Advance online articles must include the digital object identifier (DOIs) and date of initial publication.

To request permissions go to:
<http://group.bmj.com/group/rights-licensing/permissions>

To order reprints go to:
<http://journals.bmj.com/cgi/reprintform>

To subscribe to BMJ go to:
<http://group.bmj.com/subscribe/>

Notes

Advance online articles have been peer reviewed, accepted for publication, edited and typeset, but have not yet appeared in the paper journal. Advance online articles are citable and establish publication priority; they are indexed by PubMed from initial publication. Citations to Advance online articles must include the digital object identifier (DOIs) and date of initial publication.

To request permissions go to:

<http://group.bmj.com/group/rights-licensing/permissions>

To order reprints go to:

<http://journals.bmj.com/cgi/reprintform>

To subscribe to BMJ go to:

<http://group.bmj.com/subscribe/>